Progress In Electromagnetics Research, Vol. 109, 1–16, 2010

A COMPACT PLANAR MULTIBAND ANTENNA FOR INTEGRATED MOBILE DEVICES

W.-J. Liao, S.-H. Chang, and L.-K. Li

Department of Electrical Engineering
National Taiwan University of Science and Technology
43, Section 4, Keelung Road, Taipei 106, Taiwan, R.O.C.

Abstract—A compact multiband (GSM/DCS/PCS/UMTS/Bluetooth/WLANs/Wi-MAX) planar monopole antenna, which contains multiple branches, is proposed in this work. Most wireless communication bands for consumer electronics are covered in this design. The antenna radiator comprises four resonant branches on the top surface of a PCB board and one parasitic element on its back. The antenna size is 17.5 mm × 35.7 mm, and no via is needed in the fabrication process. Various techniques, such as branching, meandered lines, closed loop, capacitive coupling, parasitic elements and tapered ends, are used to enhance the antenna's bandwidth, matching and size reduction performance. Simulation and measurement show good agreement for reflection coefficient. The proposed antenna is particularly attractive for mobile devices that integrate multiple systems.

1. INTRODUCTION

Due to the success of emerging smart phone market, modern mobile communication devices tend to integrate multiple communication systems into a portable handset. Take the iPhone for example: the 4.8 ounce handset includes UMTS/HSDPA, GSM/EDGE, Wi-Fi, Bluetooth and GPS as well. Since each communication protocol may operate in a distinctive frequency band, instead of using several antennas, it is highly desirable to have one broadband or multi-band antenna to meet the antenna needs of multiple systems.

On top of the multiple band operation requirement, the smart phone antenna also needs to be compact with a low profile so that

Received 30 August 2010, Accepted 28 September 2010, Scheduled 1 October 2010
Corresponding author: Wen-Jiao Liao (wjliao@mail.ntust.edu.tw).

the antenna can be easily integrated with the circuit board and the handset enclosure. Furthermore, the antenna must provide reasonable radiation efficiency and a largely isotropic radiation pattern to ensure the connection quality.

Most current multiband antenna designs used for mobile devices can be categorized into three types: planar inverted-F antennas (PIFAs), monopole antennas and slot-type antennas. In general, a PIFA antenna contains a ground plane, a top patch, a shorting pin and a feed structure. The top patch acts as a quarter-wavelength resonator and may contain one or several slots to produce multiple resonant modes. Different techniques have been applied to PIFA design to provide multiple band operation and performance enhancement. In [1–3], L-shaped and U-shaped slots are used, while fractal apertures are added in [4] to increase the resonant path and therefore reduce the antenna size. Shorted parasitic patches with capacitive loads and slots are used in [5] to achieve multiband and wideband operations. In [6], dual band operation is achieved by inserting two long slots to provide two resonant modes, while F-shaped and rectangular slots are used to accomplish dual mode resonance in [7, 8]. In [9], a pair of slits is added to the main patch and is excited by a modified coplanar waveguide feed. In [10], an open-ended slot is cut on the ground to broaden the bandwidth. In [11], multiband operation is achieved by cutting embedded slots and via holes in the radiating patch. In [12], a PIFA antenna with electronically turnable band is achieved by adding a varactor. In summary, the PIFA antenna provides several desirable properties such as planar configuration and multiband operation while the antenna bandwidth of individual mode is limited [13] and its 3D structure may be challenging in fabrication.

The planar monopole, on the other hand, has a wider input impedance bandwidth and can easily cope with the PCB fabrication process. Multiband operation can be facilitated via several techniques. In [14–16], two or more branches, and even fractal patterns are added to the monopole design to excite multiple resonant bands. Jang and Kim implement a two branches monopole on a dielectric loading to further minimize the antenna size [17]. In [18–22], slots of various geometries are cut into the radiator and ground plane to provide multiple resonant modes. Capacitive and inductive loading/de-loading techniques are also seen in [23–29] to reduce the antenna size and increase the antenna bandwidth. Similarly, the antenna bandwidth is enhanced by the mutual coupling between the S-strips and the T-strip in [30]. Also, parallel combination of slot and PIFA are found implemented on handset antenna designs [31–33].

In this paper, a multiband antenna which covers the GSM, DCS,

PCS, UMTS, Bluetooth, WLAN and Wi-MAX is proposed. The antenna size is 17.5 mm by 35.7 mm. It comprises four branches on its top layer, while one parasitic element is added on the bottom layer. Both simulation and measurement results were provided to validate the antenna performance.

The antenna geometry and design methods are described in Section 2. Comparisons of simulated and measurement results are presented in Section 3, followed by a conclusion of this work.

2. ANTENNA DESIGN

The configuration of the proposed planar multiband antenna is illustrated in Figure 1. Table 1 lists detailed dimensions of the antenna design. The substrate used is FR4 ($\varepsilon_r = 4.4$) and the thickness is 0.8 mm. The antenna is located on the top surface of the substrate while a ground of 60 mm × 36 mm is placed on the back. A microstrip line is used to feed the antenna.

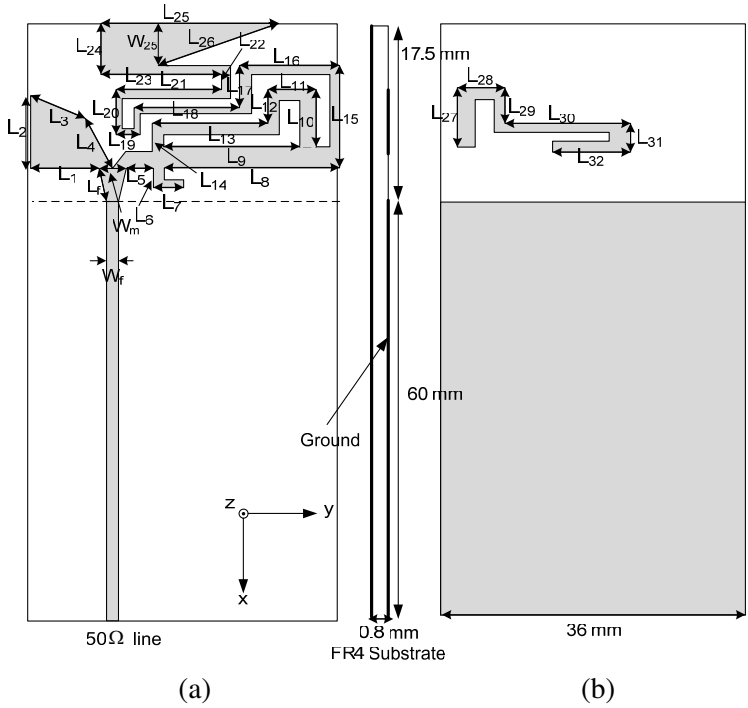

Figure 1. Configuration of the proposed multiband planar monopole antenna on a 0.8 mm FR4 substrate, (a) top view, (b) bottom view.

Table 1. Optimized antenna design dimensions (unit: mm).

L_1	9			L_{17}	4.5	W_{17}	1.5
L_2	10			L_{18}	11	W_{18}	1
L_3	6.15			L_{19}	3	W_{19}	1
L_4	8.94			L_{20}	6	W_{20}	1
L_5	3.5	W_5	1.5	L_{21}	11	W_{21}	1
L_6	2.5	W_6	2.5	L_{22}	3.5	W_{22}	1
L_7	4.2	W_7	1	L_{23}	14	W_{23}	1.5
L_8	19	W_8	2	L_{24}	7.5		
L_9	14.1			L_{25}	21	W_{25}	6
L_{10}	8	W_{10}	2.6	L_{26}	13.4		
L_{11}	7	W_{11}	1.5	L_{27}	8	W_{27}	2.76
L_{12}	4.5	W_{12}	1.5	L_{28}	7	W_{28}	1.5
L_{13}	11	W_{13}	1.5	L_{29}	4.5	W_{29}	1.5
L_{14}	3.5	W_{14}	1.3	L_{30}	12	W_{30}	1.5
L_{15}	10	W_{15}	1	L_{31}	3	W_{31}	2.24
L_{16}	12	W_{16}	1	L_{32}	8.7	W_{32}	1
L_f	4.56	W_f	1.52			W_m	3

The antenna contains four branches on the front and one parasitic element in the back. In principle, the branches operate in quarter wavelength resonance modes. The triangular branch to the left is designated to provide the Wi-MAX band (3.3–3.8 GHz) operation. Its tapered structure is used to reduce coupling with other branches. The meandered radiator to the right comprises three branches. The tiny stub near the ground is intended to operate in the higher ISM band (5.15–5.35, 5.75–5.85 GHz). The length from the feed point to the stub's end is approximately 14.7 mm, which is close to quarter wavelength in that band. The radiator to the right contains two other branches. One makes a loop in the middle while the other meandered around the perimeter of the antenna region. The long branch on the outside is used to offer the lower GSM band operation, while the middle loop is aimed to GSM/DCS/PCS/UMTS uses around 2 GHz. Strong coupling occurs between the loop and meandered branches due to close proximity. Therefore, a geometric change in one branch not only affects the resonant frequency and impedance matching in its own band, but the other bands as well. For example, by adding a wide tapered strip at the end of the meandered branch, not only the resonant frequency of the meandered branch is shifted from 1.1 GHz to 940 MHz, a better impedance matching is achieved around 2 GHz for the loop branch. Finally, the lower ISM band (2.4–2.48 GHz) operation is provided with a parasitic element attached to the back of the loop branch. This

element on the back runs in parallel with the loop on the front. Total length of sections L_{27} through L_{30} is 31.5 mm, which is close to a quarter wavelength at the desired band. Lengths and widths of end sections L_{31} and L_{32} are tuned via a simulation tool, HFSS, to optimize its matching performance. This approach eliminates the use of another branch and hence helps in antenna size reduction.

Simulations are performed to verify the effectiveness of aforementioned design approaches. Figure 2 shows that by making the middle branch as a closed loop, a relatively broad band is created between 1.5 to 2.2 GHz. Figure 3 shows the added tapered strip at the end of the meandered branch helps to lower the resonant frequencies of both upper and lower GSM bands. Figure 4 illustrates that an additional notch is created by the parasitic element.

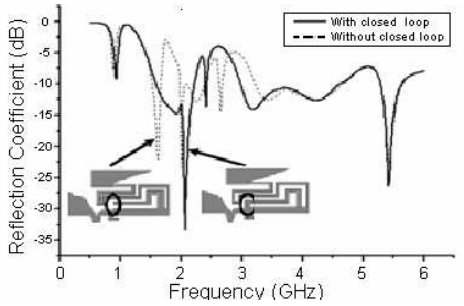

Figure 2. Comparison of reflection coefficient spectra of the proposed antenna with and without the closed loop.

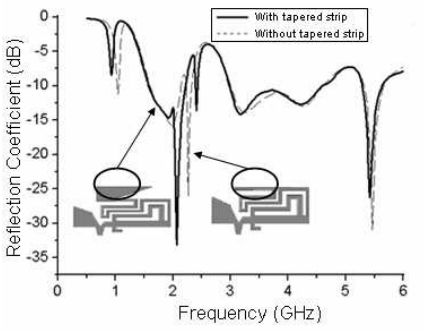

Figure 3. Comparison of the reflection coefficient spectra of the proposed antenna with and without the tapered strip.

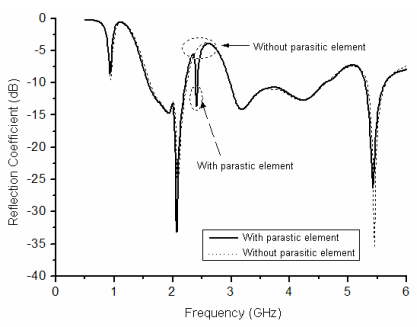

Figure 4. Comparison of reflection coefficient spectra of the proposed antenna with and without the parasitic element.

3. RESULTS AND DISCUSSION

The simulated current distributions of the multiband antenna are shown in Figure 5. At 940 MHz, the current travels mostly along the outer branch in Figure 5(a). The currents may cancel each other in region 1, so that the overall branch length is greater than one-quarter wavelength. For 1.9 GHz excitation, the current distribution has two paths as shown in Figure 5(b). Due to mutual coupling effect, the bandwidth is enhanced. For the 2.44 GHz result shown in Figure 5(c), the current is coupled from the top layer to the bottom layer. The overall current length approximates to a quarter wavelength. The 3.6 GHz current distribution shown in Figure 5(d) is concentrated on the left strip. Similar behaviour is observed for the 5.8 GHz current shown in Figure 5(e). The simulation results show that the wider strips improve the bandwidth performance in general. The fabricated prototype antenna is shown in Figure 6. The simulated and measured

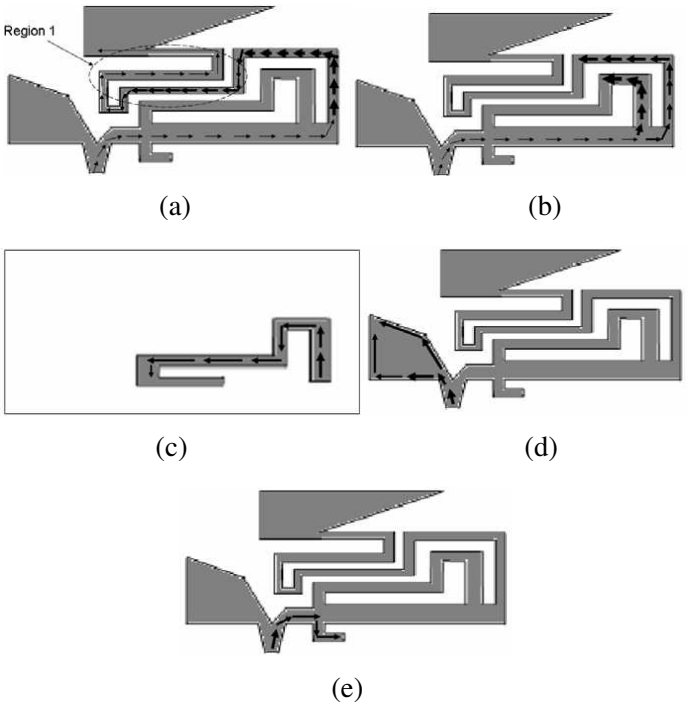

Figure 5. Simulated current distribution of the multiband antenna in application bands. (a) 940 MHz, (b) 1.9 GHz, (c) 2.44 GHz, (d) 3.6 GHz, (e) 5.8 GHz.

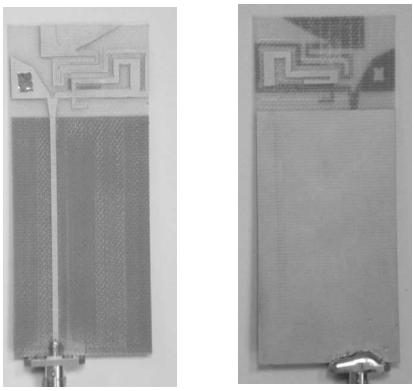

Figure 6. Fabricated multi-band antenna, (a) top layer, (b) bottom layer.

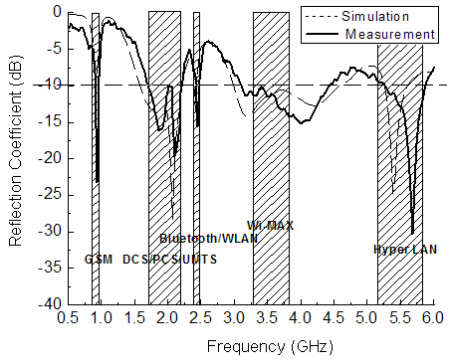

Figure 7. Simulated and measured reflection coefficient spectra of the proposed antenna.

Table 2. Gain maxima and efficiency of the proposed multiband antenna.

Applications	Resonant Frequency(GHz)	Peak Gain(dBi)	Total Efficiency(%)
GSM (890-960 MHz)	0.94 GHz	2.89 dBi	61.71 %
DCS (1.71-1.88 GHz)	1.82 GHz	3.32 dBi	68.98 %
PCS (1.85-1.99 GHz)	1.90 GHz	4.37 dBi	82.00 %
UMTS (1.92-2.17 GHz)	2.16 GHz	4.03 dBi	69.31 %
WLAN (2.4-2.48 GHz)	2.48 GHz	1.62 dBi	42.05 %
Wi-MAX (3.3-3.8 GHz)	3.60 GHz	5.15 dBi	73.31 %
WLAN (5.15-5.35 GHz)	5.15 GHz	5.91 dBi	50.52 %
WLAN (5.725-5.875 GHz)	5.85 GHz	3.52 dBi	43.07 %

reflection coefficient spectra are compared in Figure 7, which exhibit good agreements and meet the -10 dB requirement in most bands. The lowest band extends from 890 to 960 MHz to provide the lower GSM operation. DCS/PCS/UMTS bands are covered by the second resonant mode, which stretches from 1.72 to 2.3 GHz. The third band is from 2.4 to 2.48 GHz, which covers Bluetooth and WLAN uses. The

fourth band extends from 3.1 to 4.4 GHz and suffices the Wi-MAX need (3.3–3.8 GHz) in Europe. Finally, the fifth band, which begins from 5.15 to 5.86 GHz, covers the upper ISM band.

The radiation patterns were measured in a 3D spherical nearfield chamber. Co- and cross-polarization radiation patterns on XY-, XZ- and YZ-planes are exhibited in Figure 8 to Figure 15 for various frequencies. Below 2.5 GHz, the antenna is relatively small in terms of wavelength. The radiation patterns are in general isotropic without preferred plane or polarization. The YZ-plane patterns are somewhat omnidirectional at 1.82, 1.9 and 2.48 GHz. At higher frequency bands, the antenna structure becomes larger electrically. The measured patterns are volatile with apparent nulls on specific planes. The measured antenna gain maxima and total efficiencies are tabulated in Table 2. Since reflection coefficients are less than -10 dB for most operation bands, the measured total efficiency is close to the antenna's radiation efficiency. The minimum efficiency observed is 42%, and the antenna is particularly efficient at lower bands. The corresponding peak gains confirm that the antenna is largely omnidirectional below 2.5 GHz and somewhat directive above 3.3 GHz. The highest peak gain observed is 5.91 dBi at 5.15 GHz.

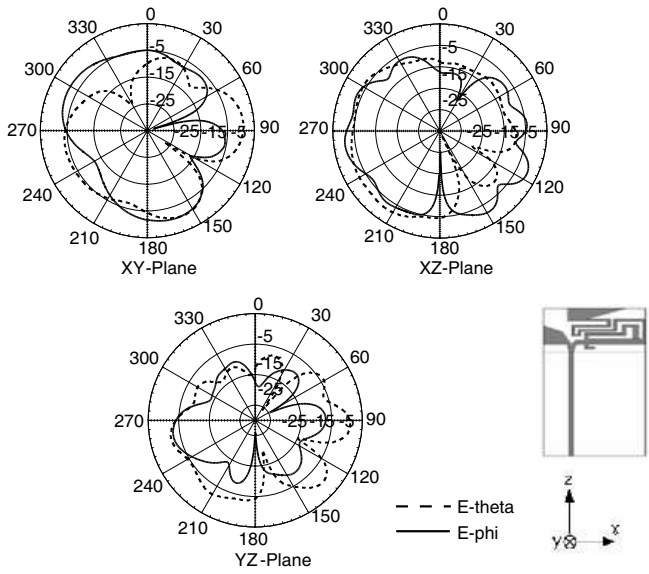

Figure 8. Measured radiation patterns of the proposed antenna at 940 MHz.

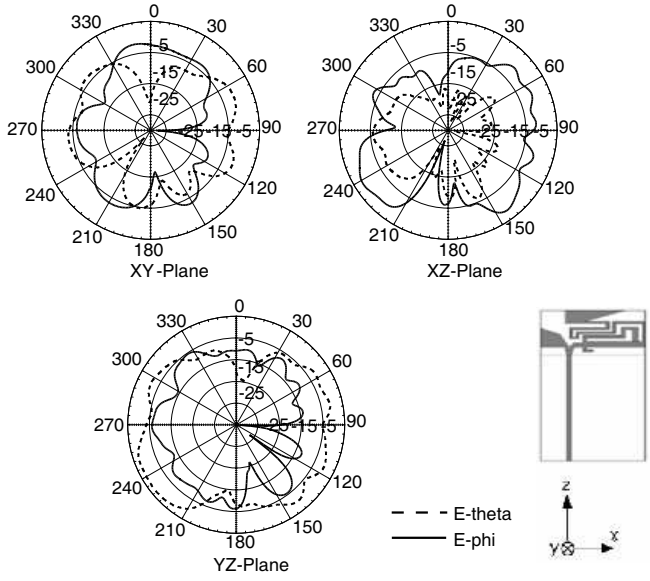

Figure 9. Measured radiation patterns of the proposed antenna at 1.82 GHz.

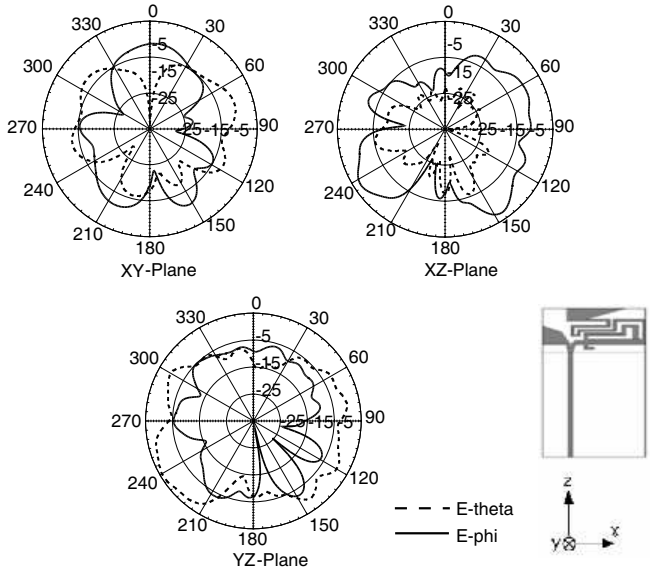

Figure 10. Measured radiation patterns of the proposed antenna at 1.9 GHz.

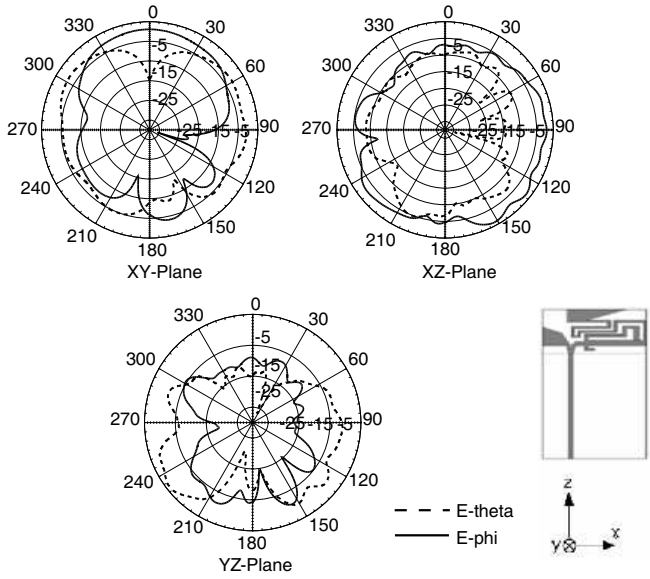

Figure 11. Measured radiation patterns of the proposed antenna at 2.16 GHz.

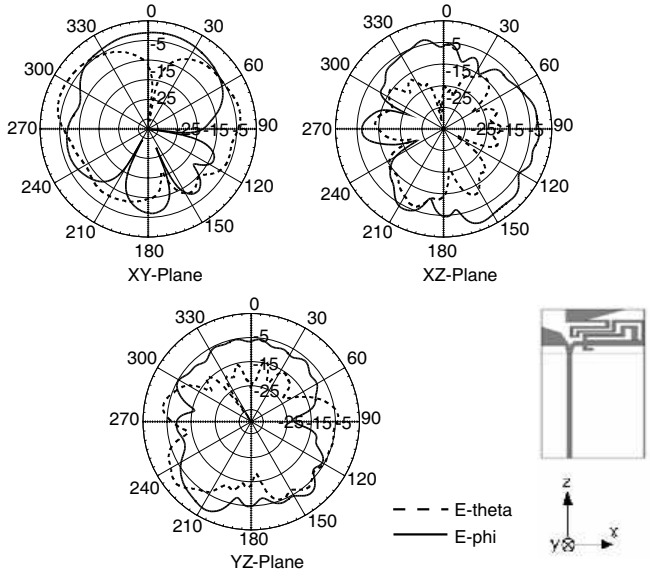

Figure 12. Measured radiation patterns of the proposed antenna at 2.48 GHz.

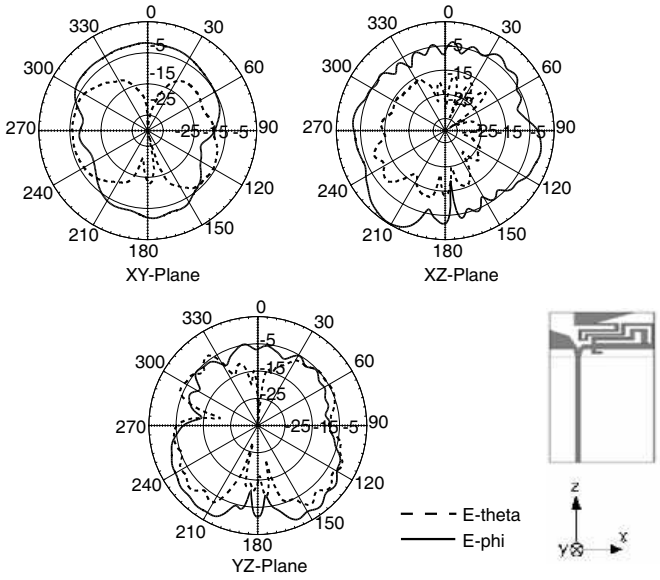

Figure 13. Measured radiation patterns of the proposed antenna at 3.6 GHz.

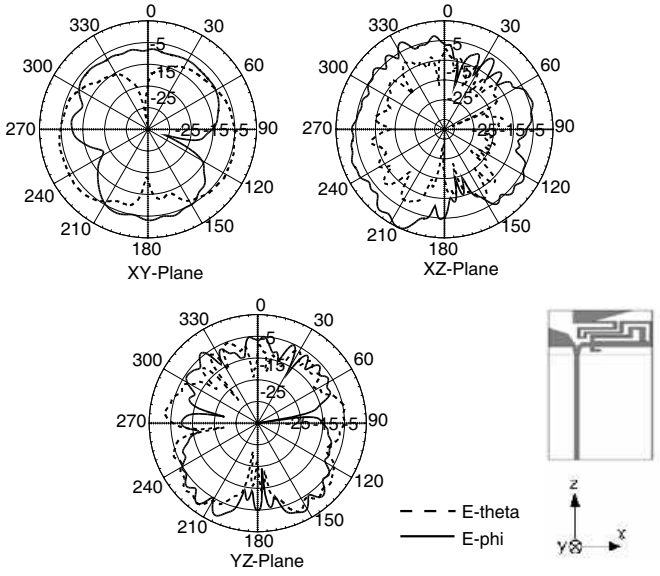

Figure 14. Measured radiation patterns of the proposed antenna at 5.15 GHz.

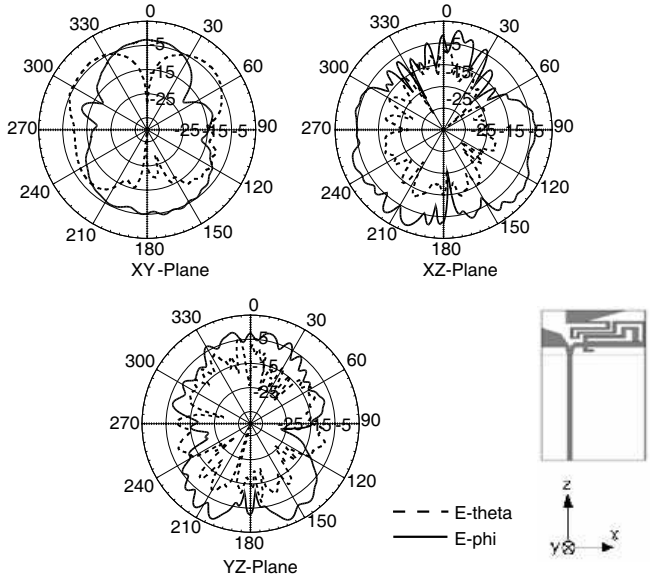

Figure 15. Measured radiation patterns of the proposed antenna at 5.85 GHz.

Above results demonstrate that the proposed antenna, which is based on the monopole configuration, provides good radiation efficiency and isotropic radiation patterns in most bands. Nevertheless, the monopole antenna configuration, which utilizes the ground as part of its radiator, is in general susceptible to coupling from nearby objects. Therefore we performed a couple of reflection coefficient measurements with the PCB test bench held by hand or placed near the human head. Figure 16(a) compares the baseline measurement, which is done without nearby obstruction, and the one with a hand holding the lower part of the test bench. Plots show that except bands near 2 GHz, which are generated from the branch nearest to the ground, other bands suffer only limited shifts and matching performance degradation. These results show the proposed design, which places all antenna branches as farther away from the hand as possible, is resilient to interference from the user's body at a certain degree. Figure 16(b) presents the result of placing another metal sheet, which is as large as the ground plane, behind the PCB board by 10 mm. The curve makes little difference to the baseline result. This result indicates the device enclosure, which may contain some conducting parts, should be included in the design tuning phase to ensure that interaction between the antenna and the user is limited and the radiation toward user's head is suppressed.

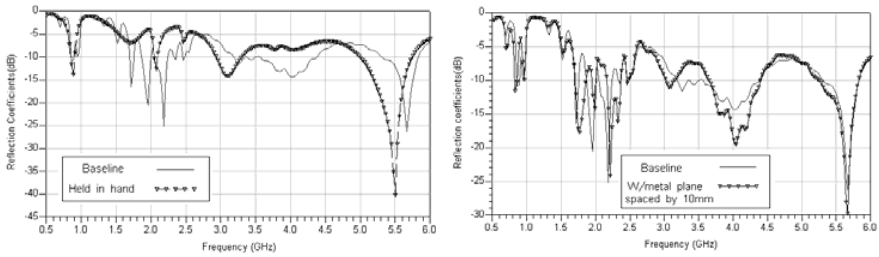

(a) (b)

Figure 16. Measured reflection coefficient spectra of various test bench setups. (a) baseline and test bench held in hand, (b) baseline and a metal plane placed behind test bench by 10 mm.

4. CONCLUSION

A compact planar multiband antenna based on the multi-branch monopole configuration is developed in this work. The measured return spectrum complies with the frequency needs of GSM, DCS, PCS, UMTS, Bluetooth, WLAN and WiMAX applications. The proposed antenna design exhibits a compact size and largely omnidirectional radiation patterns. Since the antenna can be integrated with the PCB board and occupies a small area, it is particularly attractive for portable devices such as smart phones and PDAs.

REFERENCES

1. Bhatti, R.-A., Y.-S. Shin, N.-A. Nguyen, and S.-O. Park, "Design of a novel multiband planar inverted-F antenna for mobile terminals," *Proceedings IEEE IWAT*, 226–229, 2008.
2. Nashaat, D. M., H. A. Elsadek, and H. Ghali, "Single feed compact quad-band PIFA antenna for wireless communication applications," *IEEE Trans. Antennas Propag.*, Vol. 53, No. 8, 2631–2635, Aug. 2005.
3. Lin, D.-B., I-T. Tang, and M.-Z. Hong, "A compact quad-band PIFA by tuning the defected ground structure for mobile phones," *Progress In Electromagnetics Research B*, Vol. 24, 173–189, 2010.
4. Saidatul, N. A., A. A. H. Azremi, R. B. Ahmad, P. J. Soh, and F. Malek, "Multiband fractal planar inverted F antenna (F-PIFA) for mobile phone application," *Progress In Electromagnetics Research B*, Vol. 14, 127–148, 2009.
5. Ciais, P., R. Staraj, G. Kossiavas, and C. Luxey, "Compact

internal, multiband antenna for mobile phone and WLAN standards," *Electron. Lett.*, Vol. 40, No. 15, Jul. 2004.

6. Han, M.-S. and H.-T. Kim, "Compact five band internal antenna for mobile phone," *IEEE Antennas and Propagation Society International Symposium*, 4381–4384, Jul. 2006.
7. Anguera, J., A. Cabedo, C. Picher, I. Sanz, M. Ribó, and C. Puente "Multiband handset antennas by means of groundplane modification," *IEEE Antennas and Propagation Society International Symposium*, 1253–1256, Jun. 2007.
8. Guo, Y.-X., I. Ang, and M. Y. W. Chia, "Compact internal multiband antennas for mobile handsets," *IEEE Antennas Wireless Propag. Lett.*, Vol. 2, 143–146, 2003.
9. Park, H., K. Chung, and J. Choi, "Design of a planar inverted-F antenna with very wide impedance bandwidth," *IEEE Microw. Wirelss Compon. Lett.*, Vol. 16, No. 3, 113–115, Mar. 2006.
10. Lin, D.-B., I.-T. Tang, M.-Z. Hong, and H.-P. Lin, "A compact quad-band PIFA by using defected ground structure," *IEEE Antennas and Propagation Society International Symposium*, 4677–4680, Jun. 2007.
11. Kwak, W.-I., S.-O. Park, and J.-S. Kim, "A folded planar inverted-F antenna for GSM/DCS/Bluetooth triple-band application," *IEEE Antennas Wireless Propag. Lett.*, Vol. 5, 18–21, Dec. 2006.
12. Liang, J. and H. Y. D. Yang, "Varactor loaded tunable printed PIFA," *Progress In Electromagnetics Research B*, Vol. 15, 113–131, 2009.
13. Hua, R.-C., C.-F. Chou, S.-J. Wu, and T.-G. Ma, "Compact multiband planar monopole antennas for smart phone applications," *IET Microwaves, Antennas & Propagation*, Vol. 2, 473–481, Aug. 2008.
14. Jaw, J.-L. and J.-K. Chen, "CPW-fed hook-shaped strip antenna for dual wideband operation," *Journal of Electromagnetic Waves and Applications*, Vol. 22, No. 13, 1809–1818, 2008.
15. Xiong, J.-P., L. Liu, X.-M. Wang, J. Chen, and Y.-L. Zhao, "Dual-band printed bent slots antenna for WLAN applications," *Journal of Electromagnetic Waves and Applications*, Vol. 22, No. 11–12, 1509–1515, 2008.
16. Mahatthanajatuphat, C., S. Saleekaw, and P. Akkaraekthalin, "A Rhombic patch monopole antenna with modified Minkowski fractal geometry for UMTS, WLAN, and mobile WiMAX application," *Progress In Electromagnetics Research*, Vol. 89, 57–

74, 2009.

17. Jang, B. C. and C. Y. Kim, "Internal antenna design for a triple band using an overlap of return loss," *Journal of Electromagnetic Waves and Applications*, Vol. 21, No. 8, 1099–1108, 2007.
18. Wong, K.-L., G.-Y. Lee, and T.-W. Chiou, "A low-profile planar monopole antenna for multiband operation of mobile handsets," *IEEE Trans. Antennas Propag.*, Vol. 51, 121–125, Jan. 2003.
19. Ge, Y., K. P. Essells, and T. S. Bird, "A spiral-shaped printed monopole antenna for mobile communications," *IEEE Antennas and Propagation Society International Symposium*, 3681–3684, Jul. 2006.
20. Liu, C.-S., C.-N. Chiu, and S.-M. Deng, "A compact disc-slit monopole antenna for mobile devices," *IEEE Antennas Wireless Propag. Lett.*, Vol. 7, 251–254, 2008.
21. Jing, X., Z. Du, and K. Gong, "A compact multiband planar antenna for mobile handsets," *IEEE Antennas Wireless Propag. Lett.*, Vol. 5, 343–345, Dec. 2006.
22. Lin, C.-I. and K.-L. Wong, "Printed monopole slot antenna for internal multiband mobile phone antenna," *IEEE Trans. Antennas Propag.*, Vol. 55, 3690–3697, Dec. 2007.
23. Wang, H. and M. Zheng, "Triple-band wireless local area network monopole antenna," *IET Microwaves, Antennas & Propagation*, Vol. 2, 367–372, Jun. 2008.
24. Li, R., B. Pan, J. Laskar, and M. M. Tentzeris, "A compact broadband planar antenna for GPS, DCS-1800, IMT-2000, and WLAN applications," *IEEE Antennas Wireless Propag. Lett.*, Vol. 6, 25–27, 2007.
25. Zhang, G.-M., J. S. Hong, B.-Z. Wang, Q. Y. Qin, J. B. Mo, and D.-M. Wan, "A novel multi-folded UBW antenna fed by CPW," *Journal of Electromagnetic Waves and Applications*, Vol. 21, No. 14, 2109–2119, 2007.
26. Liu, W.-C. and H.-J. Liu, "Miniaturized asymmetrical CPW-fed meandered strip antenna for triple-band operation," *Journal of Electromagnetic Waves and Applications*, Vol. 21, No. 8, 1089–1097, 2007.
27. Jamalpoo, R., J. Nourinia, and C. Ghobadi, "A wideband microstrip-fed monopole antenna for WiBro, WLAN, DMB and UWB applications," *Journal of Electromagnetic Waves and Applications*, Vol. 22, No. 11–12, 1461–1468, 2008.
28. Zhao, G., F.-S. Zhang, Y. Song, Z.-B. Weng, and Y.-C. Jiao, "Compact ring monopole antenna with double meander lines for

2.4/5 GHz dual-band operation," *Progress In Electromagnetics Research*, Vol. 72, 187–194, 2007.

29. Yin, X.-C., C.-L. Ruan, S.-G. Mo, C.-Y. Ding, and J.-H. Chu, "A compact ultra-wideband microstrip antenna with multiple notches," *Progress In Electromagnetics Research*, Vol. 84, 321–332, 2008.
30. Tung, H.-C. and Y.-C. Hsu, "Monopole antenna fed by a coaxial cable in slide phone for GSM/DCS/PCS operation," *IEEE Antennas and Propagation Society International Symposium*, 1–4, Jul. 2008.
31. Anguera, J., I. Sanz, A. Sanz, A. Condes, D. Gala, C. Puente, and J. Soler, "Enhancing the performance of handset antennas by means of ground plane design," *IEEE International Workshop on Antenna Technology: Small Antennas and Novel Metamaterials (IWAT 2006)*, New York, USA, Mar. 2006.
32. Cabedo, A., J. Anguera, C. Picher, M. Ribó, and C. Puente, "Multi-band handset antenna combining a PIFA, slots, and ground plane modes," *IEEE Trans. Antennas Propag.*, Vol. 57, No. 9, 2526–2533, Sep. 2009.
33. Anguera, J., I. Sanz, J. Mumbrú, and C. Puente, "Multi-band handset antenna with a parallel excitation of PIFA and slot radiators," *IEEE Trans. Antennas Propag.*, Vol. 58, No. 2, 348–356, Feb. 2010.